Responses of MST neurons to plaid stimuli

Farhan A. Khawaja, Liu D. Liu, and Christopher C. Pack
Montreal Neurological Institute, McGill University, Montreal, Quebec, Canada

Khawaja FA, Liu LD, Pack CC. Responses of MST neurons to
plaid stimuli. *J Neurophysiol* 110: 63–74, 2013. First published April
17, 2013; doi:10.1152/jn.00338.2012.—The estimation of motion
information from retinal input is a fundamental function of the
primate dorsal visual pathway. Previous work has shown that this
function involves multiple cortical areas, with each area integrating
information from its predecessors. Compared with neurons in the
primary visual cortex (V1), neurons in the middle temporal (MT) area
more faithfully represent the velocity of plaid stimuli, and the obser-
vation of this pattern selectivity has led to two-stage models in which
MT neurons integrate the outputs of component-selective V1 neurons.
Motion integration in these models is generally complemented by
motion opponency, which refines velocity selectivity. Area MT proj-
ects to a third stage of motion processing, the medial superior
temporal (MST) area, but surprisingly little is known about MST
responses to plaid stimuli. Here we show that increased pattern
selectivity in MST is associated with greater prevalence of the
mechanisms implemented by two-stage MT models: Compared with
MT neurons, MST neurons integrate motion components to a greater
degree and exhibit evidence of stronger motion opponency. Moreover,
when tested with more challenging unikinetic plaid stimuli, an appre-
ciable percentage of MST neurons are pattern selective, while such
selectivity is rare in MT. Surprisingly, increased motion integration is
found in MST even for transparent plaid stimuli, which are not
typically integrated perceptually. Thus the relationship between MST
and MT is qualitatively similar to that between MT and V1, as
repeated application of basic motion mechanisms leads to novel
selectivities at each stage along the pathway.

motion integration; vision; electrophysiology; perception; cortex

MOTION PERCEPTION IS CRITICAL for a variety of tasks, from the
moment-to-moment stabilization of gaze (Miles 1997) to suc-
cessful performance in professional sports (Regan 1997). In the
primate brain, motion processing is carried out by a collection
of dedicated cortical areas, all of which receive direct or
indirect input from the primary visual cortex (V1).

Although clear selectivity for stimulus motion is found in V1
(Hubel and Wiesel 1962), the ability of individual V1 neurons
to estimate velocity for many types of stimuli is severely
limited. Part of this limitation is due to the fact that V1
receptive fields are quite small, so that they only signal the
motion of an object as it passes through a roughly 1° region of
visual space. Thus in natural vision V1 neurons are generally
able to provide only momentary information on a moving
object's velocity, and even this information is quite limited by
the structure of the environment: Objects are usually composed
of edges for which local motion computations can only recover
the component of motion perpendicular to the orientation of the
edge (Wallach 1935). Because most V1 neurons are highly
selective for such orientation cues, their outputs are in many

cases ambiguous with respect to the velocity of the stimulus.
Thus while V1 appears to be necessary for motion perception,
its outputs are not sufficient to support accurate motion per-
ception for the kinds of stimuli typically encountered in a
natural environment.

Area V1 projects to a variety of extrastriate visual regions
that are likely to be involved in motion perception. Here we
focus on the properties of the projection to the middle temporal
(MT) area, which is highly specialized for motion processing.
MT appears to be capable of overcoming many of the ambi-
guities present in the V1 output (Albright 1984; Movshon et al.
1985), and consequently it has inspired a number of two-stage
models of motion processing. These models have converged on
a number of key computational mechanisms for integrating
motion signals (Rust et al. 2006; Simoncelli and Heeger 1998;
Tsui et al. 2010). The first is a motion-opponent mechanism
that removes information about static orientation cues by
subtracting the outputs of neurons that share the same motion
preference but opposite motion directions (Adelson and Bergen
1985; Reichardt 1961; Rust et al. 2006; Simoncelli and Heeger
1998). The second is a pooling mechanism that incorporates
information from multiple motion components by summing the
responses of V1 neurons tuned to different orientations (Rust et
al. 2006; Simoncelli and Heeger 1998; Tsui et al. 2010). These
models also contain nonlinear mechanisms that have been
explored in detail elsewhere (Tsui et al. 2010).

These basic motion processing mechanisms can be probed
with plaid stimuli (Fig. 1A) that are composed of two grating
components, each of which moves in a different direction.
Such stimuli are typically perceived by humans to be moving
in a direction corresponding to neither grating but rather to a
velocity consistent with both of the one-dimensional grating
components (Adelson and Movshon 1982). In contrast to these
perceptual findings, V1 neurons generally respond to the indi-
vidual component gratings (Movshon et al. 1985) and carry
very little information about the motion of the plaid pattern. A
subpopulation of MT neurons is capable of signaling the
motion of the plaid pattern (Movshon et al. 1985), and this
capability is associated with both stronger evidence of motion
opponency and a broader integration of motion components
(Rust et al. 2006).

Although these experimental and computational results sug-
gest a clear distinction between areas V1 and MT, very little is
known about the response of neurons in higher areas to plaid
stimuli. Indeed, a subsequent stage of motion processing, the
medial superior temporal area (MST), has primarily been
studied with complex optic flow patterns (Duffy and Wurtz
1991b; Saito et al. 1986; Tanaka et al. 1986), so that its role in
the basic integration of motion information is less clear. We
have therefore recorded the responses of neurons in MST to a
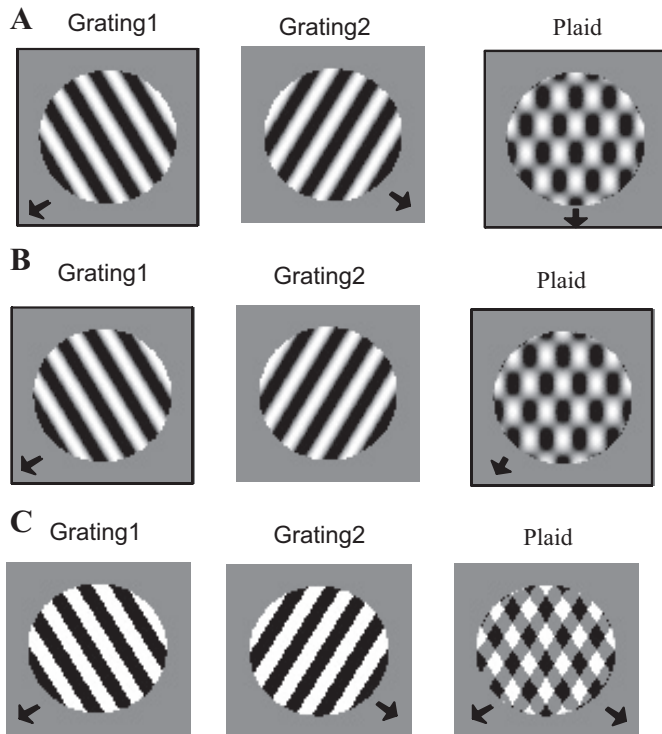variety of plaid stimuli that have classically been used to study

Fig. 1. Experimental stimuli. *A*: examples of bikinetic stimuli used in our experiments. Cells were stimulated with both a single grating (*left* and *center*) and a plaid stimulus (*right*) formed by summing 2 gratings with orientations that differed by 120°. Arrows represent the direction perceived by human observers. *B*: unikinetic plaid stimuli in which only 1 of the gratings moves (*left*) while the other remains stationary (*center*). The perceived direction is parallel to the orientation of the stationary grating (arrow, *right*). *C*: transparent plaid stimuli (*right*) consisting of two square gratings (*left* and *center*). The motion of both gratings is typically perceived (arrows, *right*).

V1, MT, and visual perception. Our results indicate that area MST carries out some of the basic functions typically assigned to the second stage of the two-stage model. These include the suppression of information about static orientation (consistent with a motion-opponent mechanism) and the generalization of motion processing across one-dimensional components (pooling). Surprisingly, MST neurons are relatively insensitive to nonmotion cues that are associated with perceptual transparency, suggesting that many neurons at higher levels of the dorsal hierarchy obligatorily integrate motion signals in a way that is not necessarily consistent with human perception.

Overall our results, while consistent with the hierarchical basis of two-stage models of motion processing, suggest a more general set of computations that are shared across all cortical areas. These include simple mechanisms for pooling of outputs across space and across feature selectivity and for suppressing irrelevant input signals. We speculate that these generic mechanisms, along with additional nonlinear mechanisms characterized elsewhere (Mineault et al. 2012), are likely to be at work in other parts of the visual cortex (Cadieu et al. 2007; Connor et al. 2007; Rust and Dicarlo 2010).

METHODS

Electrophysiological recordings. Three rhesus macaque monkeys took part in the experiments. Prior to the experiments each animal underwent a sterile surgical procedure to implant a headpost and a recording cylinder, and after recovery monkeys were seated comfort-

ably in a primate chair (Crist Instruments) and trained to fixate a small red spot on a computer monitor in return for a liquid reward. Eye position was monitored at 200 Hz with an infrared camera (SR Research) and required to be within 2° of the fixation point in order for the reward to be dispensed. All aspects of the experiments were approved by the Animal Care Committee of the Montreal Neurological Institute and were in compliance with regulations established by the Canadian Council on Animal Care.

We recorded from well-isolated single neurons in areas V1, MT, and MST. Single waveforms were sampled at 40 kHz, sorted online, and then resorted off-line with spike-sorting software (Plexon). Area MT was identified on the basis of anatomical MRI scans, the prevalence of direction-selective neurons, and the correlation between receptive field size and eccentricity. Area MST was always found to be a few millimeters past MT during a posterior approach, with a gap in audible neural activity as the electrode tip passed through the superior temporal sulcus. MST cells generally had larger receptive fields that often extended into the ipsilateral visual field (Saito et al. 1986); many of these responded selectively to expanding and/or rotating stimuli in addition to the translating stimuli used in the tests of pattern selectivity. These neurons were analyzed in detail in a recent paper (Mineault et al. 2012).

It has been shown that both MT and the lateral/ventral portion of MST (MSTl) exhibit strong surround-suppression (Born 2000; Eifuku and Wurtz 1998), while MSTd neurons are generally not surround-suppressed. We generated area summation curves for many of the MT and MST neurons in our sample, based on responses to random dot stimuli moving at the preferred velocity for each neuron. To quantify these results, we used a surround-suppression index, which quantifies the extent to which a neuron is suppressed by stimuli that are presented beyond the size of its classical receptive field. In our data we found that the surround-suppression index of our MST sample was significantly lower than that of our MT sample (median surround-suppression index = 0.48 for MST vs. 0.64 for MT; $P = 0.009$; Student's t-test). However, it has been shown that MSTl neurons exhibit surround-suppression that is on average greater than that of MT neurons (Eifuku and Wurtz 1998). Overall, these results suggest that most of our recordings were from the dorsal, rather than the ventral, portion of MST, although this has not been verified histologically.

Local field potentials (LFPs) and single units (SUs) were recorded simultaneously on the same electrodes. LFPs were filtered with an analog two-pole low-cut (0.7 Hz) and a four-pole high-cut (170 Hz) filter (Plexon) and were then digitized and sampled at 1 kHz; 60-Hz line noise was removed online with a software-switchable analog two-pole low-cut filter (Plexon). However, the power spectra of a number of LFP traces still showed a peak at 60 Hz and its first harmonic. Thus we removed this noise off-line by applying a Gaussian notch filter (width = 5 Hz) whose peak corresponded to the peak of the line noise.

Procedure and visual stimuli. Stimuli were displayed at 85 Hz at a resolution of 1,920 × 1,200 pixels. The viewing area subtended 70° × 42° of visual angle at a distance of 42 cm. Sinusoidal gratings were displayed on a gray background (luminance of 70.3 cd/m²); bikinetic plaids were constructed by superimposing two gratings of 50% contrast that differed in motion direction by 120°. Unikinetic plaids made use of the same grating components, but one component remained stationary throughout each trial. For the experiments involving transparent plaids, square-wave gratings (luminance of 81 cd/m²) were displayed on a gray background (luminance of 106 cd/m²). Coherent plaids were then constructed by summing two gratings whose motion directions differed by 120°. We then tested each neuron again with similar square-wave gratings (luminance of 148 cd/m²) against a background of 248 cd/m². Transparent plaids were constructed by combining two gratings such that the luminance of the intersections was 88 cd/m², which effectively simulated conditions in which transparent gratings (transmittance ~60%) moved in front of a
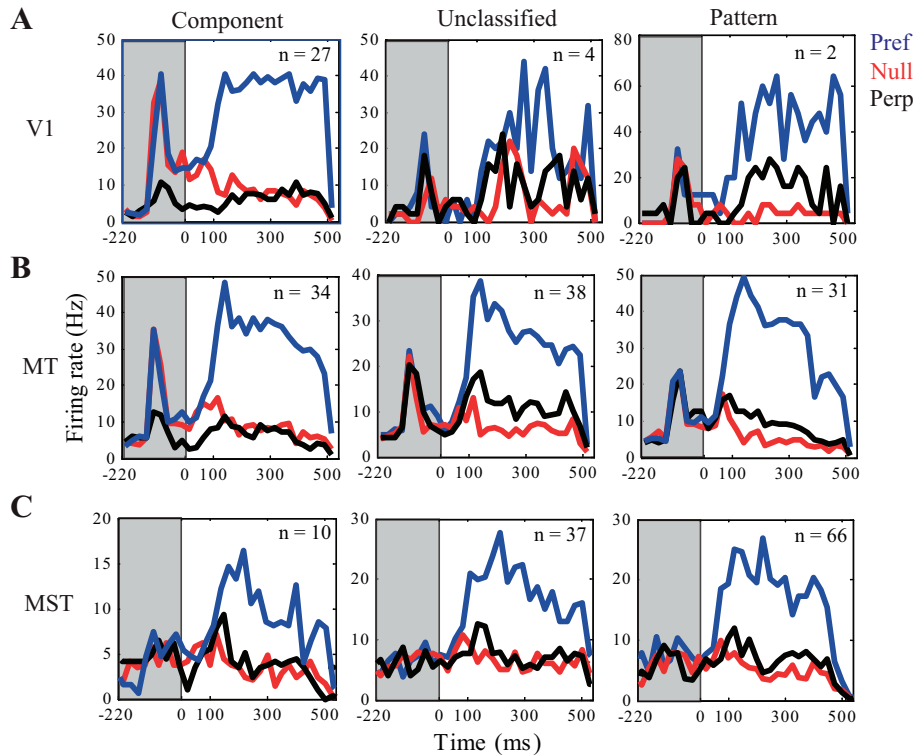
Fig. 2. Mean peristimulus time histograms (PSTHs) for primary visual cortex (V1; $n = 33$), middle temporal area (MT; $n = 103$), and medial superior temporal area (MST; $n = 113$). *A*: PSTHs for V1 showing mean spike responses evoked using grating stimuli for the group of component (*left*), unclassified (*center*) and pattern (*right*) neurons in our sample. Preferred (Pref), null, and perpendicular (Perp) directions are shown. Gratings were presented at −200 ms, remained stationary for 200 ms, and then began moving at 0 ms. The response evoked by the stationary stimulus is highlighted in gray. *B*: PSTHs for MT. *C*: PSTHs for MST.

light source. Consequently they were well within the "transparency zone" defined by Stoner et al. (1990), and their appearance was judged informally to be transparent by human observers.

For all stimuli, spatial frequency, temporal frequency, and stimulus size were optimized for each cell. Motion direction was sampled in 30° steps. On each trial the animal was required to acquire and then maintain fixation for 250 ms, after which the stimulus appeared and remained stationary for 200 ms. The stimulus then moved at a constant direction and speed for 500 ms. Each stimulus was repeated five times in blockwise random order.

Data analysis. Measurements of direction selectivity were taken from spikes averaged over a time period that spanned 120–500 ms after the onset of stimulus motion. This time period was chosen to exclude the early period when the component/pattern classification changes in many cells (Pack et al. 2001). From the resulting spike rate we subtracted the spontaneous activity measured during the 250 ms between the acquisition of fixation and the onset of the stimulus. Spike tuning curves were considered direction selective if their directionality index (DI = preferred direction response/null direction response) was >2. We also fitted the direction tuning curves to a Gaussian function, using the Levenberg-Marquardt method in the MATLAB optimization toolbox (MathWorks, Natick, MA), and required the fit to be well characterized ($r^2 > 0.95$). Recordings that did not meet these criteria were excluded from further analysis. By optimizing the fit of each direction tuning curve to a Gaussian function, we obtained several parameters, including preferred direction, baseline firing rate, amplitude of response to preferred direction, and variance. The bandwidths of the tuning curves were obtained by multiplying the standard deviation of the best-fitting Gaussian by $\sqrt{2\pi}$.

LFP responses were quantified by measuring their mean power, which was computed from the discrete Fourier transform function in MATLAB. We only included those LFP responses whose mean power for any given frequency bin was at least two standard deviations greater than the mean power of spontaneous activity.

To generate peristimulus time histograms (e.g., Fig. 2), we used a 20-ms bin size. For the analysis of onset responses, we only considered neurons with an average motion response of >10 spikes/s. The onset response was quantified as the maximum response in any 32-ms bin before stimulus motion onset. In other words, it was the firing rate corresponding to the time bin that contained the maximum response to the static stimulus. The motion response was defined as the average response of a neuron to grating motion 120–500 ms after motion onset. We also computed a static response index, which was defined as the ratio of the onset response to the motion response (Fig. 3*A*). Thus static response indexes tended to be higher for those cells that had larger responses to static stimuli relative to moving stimuli.
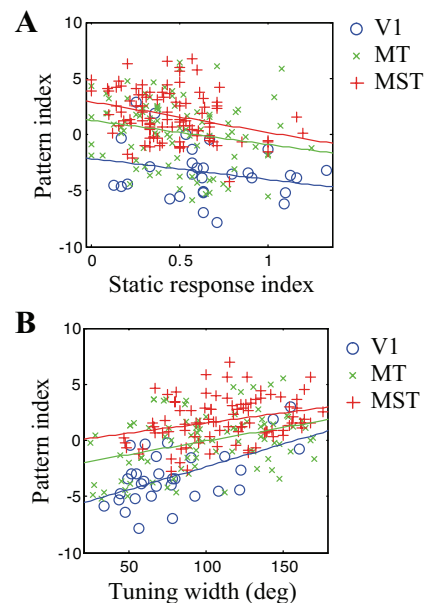

Fig. 3. Correlations of pattern index (PI) vs. static response index and tuning width for V1, MT, and MST. *A*: scatterplot showing the correlation between PI and static response index for V1, MT, and MST. Solid lines show the linear fits obtained with an ANCOVA model. *B*: scatterplot illustrating the correlation between PI and motion tuning bandwidth for V1, MT, and MST.

Spike responses to gratings and plaids were classified according to the Z-transformed partial correlation coefficients between the data and the component and pattern predictions (Smith et al. 2005; Tinsley et al. 2003) with the following equations (shown for the Z-transformed pattern correlation):

$$Z_p = 0.5 \times \ln\left[\frac{(1 + PC_p)/(1 - PC_p)}{\sqrt{1/(n-3)}}\right] \tag{1}$$

where n corresponds to the number of motion directions (12 in our experiments) and PC_p is defined as follows:

$$PC_p = \frac{(RC_p - RC_c RC_{cp})}{\sqrt{(1 - RC_c^2)(1 - RC_{cp}^2)}} \tag{2}$$

Here RC_p and RC_c are the raw correlations between the data and the pattern prediction and component predictions, respectively, and RC_{cp} is the raw correlation between the two predictions. The Z-transformed component correlation (Z_c) can be obtained by exchanging PC_p and PC_c, and the partial correlation (PC_c) between the component prediction and the data can be obtained by replacing RC_p with RC_c in the above equations. Each of the Z-transformed values was tested for significance according to the criterion of 1.28, equivalent to $P = 0.10$. The pattern index (PI) was defined for each cell as $Z_p - Z_c$, and the component index was defined to be $Z_c - Z_p$.

For the experiments involving transparent plaids, a transparency index (TI) was used to quantify the amount of transparency modulation for each cell. The transparency index was mathematically defined to be the component index obtained with the coherent plaid stimulus subtracted from the component index obtained with the transparent plaid. Higher values of the transparency index represent higher transparency modulation for a particular neuronal response.

To illustrate how PI changes over time in MT and MST, we used a 10-ms bin size and analyzed neuronal responses incrementally, beginning at 60 ms after stimulus motion onset (see Fig. 7). For example, the first bin used to calculate PI was 60–70 ms while the second bin was 60–80 ms. We considered a neuron to exhibit pattern (or component) selectivity when it remained pattern tuned (or component tuned) for five consecutive time bins. The emergence of pattern selectivity was considered to be the first of these time bins.

To determine the surround-suppression index for each neuron, we first computed the ratio of the neuronal response evoked by the largest stimulus size to the largest neuronal response (for all the different stimulus sizes tested). This result was subtracted from 1 to generate the surround-suppression index.

Models used to predict unikinetic plaid responses. We used two different methods to compute the component predictions for unikinetic plaids. In the first method (corresponding to Fig. 5), we considered only the moving grating to compute the component prediction. For this model prediction we ignored the responses to the static grating under the assumption that these responses are generally much smaller than those elicited by a moving grating. However, a more accurate component prediction may be formed by considering the responses to the static grating as well, simply because a unikinetic plaid stimulus contains a static grating as one of its components. Estimates of the neuronal response to the static grating were taken from the period of each trial in which the grating remained stationary for 200 ms.

One problem with our approach to estimating the contribution of static orientation cues is that the response to the static grating is subject to contrast gain control, which varies over time and with the presence of the second grating of the plaid. Consequently, it is difficult to isolate the contribution of static orientation cues to the responses to unikinetic plaids. To ensure that the variable gain of this response did not bias our results, we performed a second analysis in which the gain of the static grating response was treated as a free parameter, according to

$$CP = \left[R_{GM} + (R_{GO} \times g)\right] \tag{3}$$

where CP is the component prediction, R_{GM} is the response to grating movement, R_{GO} is the response to grating orientation, and g is the free parameter corresponding to the gain of the static grating (orientation) response. By fitting this equation to the data obtained with unikinetic plaids, we obtained an upper bound on the validity of the component prediction for variations in the gain of the orientation response.

The pattern motion prediction for unikinetic plaids was generated by rotating the neuronal response to the grating stimulus clockwise by 30° (Ferrera and Wilson 1990). This direction was along the orientation of the static grating and corresponded to the velocity that would be associated with the plaid if it were a single, rigidly moving object.

RESULTS

We recorded from a total of 335 neurons in areas V1, MT, and MST of three alert macaque monkeys. All neurons were categorized according to their responses to the plaid stimuli shown in Fig. 1*A*. These bikinetic plaid stimuli consist of two superimposed sinusoidal gratings, each of which moves in a different direction; these component directions are distinct from the pattern direction, which is the motion of the pattern as a whole. This distinction, along with standard statistical analysis (see METHODS), permits a classification of each neuron according to its ability to integrate motion components. Neurons that respond predominantly to the motion of the plaid pattern are called pattern selective, while those that respond to the motion components are called component selective. As described in previous work (Khawaja et al. 2009), we found that most (57%; 64/113) MST neurons were pattern selective, while such selectivity was rarer in MT (30%; 31/103) and nearly absent in V1 (6%; 2/33). In addition to these standard measures, we report here the results of experiments involving other plaid stimuli designed to answer specific questions about the integration of motion information along the dorsal pathway.

Motion opponency. Most models of motion processing implement spatial filters that are selective for stimulus orientation, based in part on the finding that direction and orientation selectivity tend to be found in the same cells in V1 (Adelson and Bergen 1985). In the time domain, these filters are often rather broadly tuned, so that they respond to stimuli of the appropriate orientation, even in the absence of motion. Motion models typically remove such orientation signals by subtracting the outputs of detectors tuned for the same orientation but opposite motion directions. This motion opponent stage has the effect of increasing direction selectivity and suppressing the responses to nondirectional noise, to which the early visual system is quite sensitive (Qian and Andersen 1994).

In our experiments each visual stimulus remained stationary for 200 ms in the receptive field of each neuron before moving. Many direction-selective neurons responded strongly during this period, despite the fact that the stimulus was stationary. Others responded weakly or not at all, which is what is expected from the output of a motion-opponent computation. To study the prevalence of these onset responses along the dorsal hierarchy, we examined responses to static gratings across the populations of component, unclassified, and pattern cells for neurons in V1, MT, and MST. The results (Fig. 2) show a robust correspondence between responses to the static stimulus and pattern selectivity. The nine panels in Fig. 2 plot the mean time course of the responses for each cell type

(component, unclassified, or pattern) and brain region (V1, MT, and MST). The onset of motion in each plot is at $t = 0$, and the stationary stimulus appears at $t = -200$. The responses evoked by stationary stimuli are highlighted in gray.

Several trends are evident in the data. First, the selectivity for static orientation is lower in pattern cells than in component cells, as shown by the fact that, on average, pattern cells respond nearly equally to orientations that are 90° apart (Fig. 2). This result is not terribly surprising, given the link between pattern selectivity and motion tuning bandwidth (Rust et al. 2006; Tinsley et al. 2003) and the links between orientation and motion tuning in V1 and MT (Albright 1984). More interesting is the relationship between the amplitudes of the responses to static orientation and pattern selectivity. Pattern cells in V1 and MT respond relatively weakly to static orientation, and in MST there is virtually no response until the stimulus starts to move. Also evident in Fig. 2 is the tendency of pattern cells from all three areas to have relatively small responses to the static orientation stimulus. These results are consistent with the suggestion (Qian and Andersen 1994; Rust et al. 2006) that motion opponency is important for pattern selectivity.

Figure 3A shows the correlation between the magnitudes of the onset responses to stationary stimuli (relative to motion responses) and the pattern index (PI), a scalar value that captures the extent to which the responses conform to the pattern prediction (see METHODS for mathematical definition). These values are shown for neurons in V1, MT, and MST. There is a significant correlation between these measures in MT ($P < 0.05$) and MST ($P < 0.01$) but not in V1 ($P = 0.18$); this latter result is likely due to the smaller sample size in V1. The slopes of the regression lines relating the magnitude of the onset response to the PI were not significantly different across areas (ANCOVA, $P > 0.60$). In contrast, the y-intercepts of these regression lines were significantly different between V1 and both MT and MST (ANCOVA, $P < 0.001$), with a marginally significant difference between MT and MST (ANCOVA, $P < 0.07$). Thus on a cell-by-cell basis, there is a relationship between the responses to stationary stimuli and the degree of pattern selectivity, and this relationship is similar across visual areas. This is consistent with the idea that the incorporation of onset transient mechanisms improves pattern selectivity in roughly the same way at all levels of the dorsal visual hierarchy. At the same time, for a given strength of onset response, pattern selectivity was stronger at higher levels of the dorsal visual hierarchy, suggesting that other factors are involved in increasing pattern selectivity in higher-level areas.

One such factor is preferred speed, which on average increases along the pathway from V1 to MT (Churchland et al. 2005; Mikami et al. 1986; Pack et al. 2006) and from MT to MST (Churchland et al. 2007; Lagae et al. 1994). Previous work (Palanca and DeAngelis 2003) has shown that some MT neurons prefer stimuli moving at speeds very close to zero, which could be related to the onset response to a nonmoving stimulus. To examine this point, we estimated the preferred speed for 40 MT neurons and 46 MST neurons. There was no significant correlation between preferred speed and pattern selectivity for either MT ($P > 0.36$) or MST ($P > 0.14$). Thus at the single-neuron level we find that the static onset response was a better predictor of pattern selectivity than preferred speed.

As an alternative to the static response measure, we also calculated the neuronal responses to motion in the antipreferred direction. In this case, a motion-opponent mechanism should produce suppression of the response below the level of spontaneous firing, as has typically been observed in MT (e.g., Mikami et al. 1986). For our sample we calculated a null-direction suppression index, which is the normalized difference between the spontaneous firing rate and the antipreferred direction firing rate. Consistent with previous models of pattern-motion processing (Rust et al. 2006; Simoncelli and Heeger 1998), there is a significant correlation between the antipreferred direction suppression index and pattern index for both MT ($P < 0.01$) and MST ($P < 0.05$). Thus both measures of motion opponency suggest that this mechanism is more effective in cells that exhibit greater pattern selectivity.

Examination of the LFPs recorded simultaneously with the single-neuron responses revealed a robust response to stimulus onset, even in area MST, where onset responses were largely absent in single neurons. Figure 4A shows the mean LFP time course, along with the mean spiking response (Fig. 4A, right), for all recording sites in MST. Here the difference between the LFP and single-neuron responses was particularly striking for the low-gamma (γ_L) frequencies (compare Fig. 4A, center and right). The peak onset response that occurs before $t = 0$ is comparable in amplitude to the peak motion response, as observed for many single-unit responses in V1 and MT (Fig. 2). Onset responses in MST were present but somewhat reduced in the high-gamma (γ_H) LFP frequencies (Fig. 4A, left).

On average, the onset responses for LFPs in MT and MST were generally similar to single-unit responses in lower-level areas (Fig. 4B), with stronger responses being found in the γ_L band than in the γ_H band. These results suggest that onset responses are stronger in the input to a given area than in the (spiking) output, as reported previously for component selectivity (Khawaja et al. 2009). One plausible explanation for both results is then that the motion-opponent mechanism, and by extension pattern selectivity, relies on lateral inhibitory connectivity, to which the LFPs are thought to be particularly sensitive (Henrie and Shapley 2005).

Bandwidth of motion integration. The previous section suggests that responses to static stimuli decrease along the dorsal pathway and that this decrease is predictive of pattern selectivity. Another measure of motion selectivity that tends to change along the motion processing hierarchy is the bandwidth of direction tuning. Neurons in V1 are quite narrowly tuned for motion direction (Gizzi et al. 1990; Hubel and Wiesel 1968; Tinsley et al. 2003), whereas those in MT and MST are more broadly tuned (Albright 1984; Duffy and Wurtz 1991a; Maunsell and Van Essen 1983). This feature would seem to be important for pattern selectivity, which requires the integration of information from motion components that move in very different directions.

Figure 3B shows the correlation between the tuning bandwidths (measured with gratings) and the PI for neurons in V1, MT, and MST. There was a significant correlation between motion tuning bandwidth and pattern selectivity in each area ($P < 0.01$ for MST, $P < 0.001$ for MT, and $P < 0.01$ for V1). As shown above for motion onset responses, the slopes of the regression lines relating tuning bandwidth to pattern selectivity were not significantly different across areas (ANCOVA, $P > 0.12$). The y-intercepts of these regression lines were significantly different
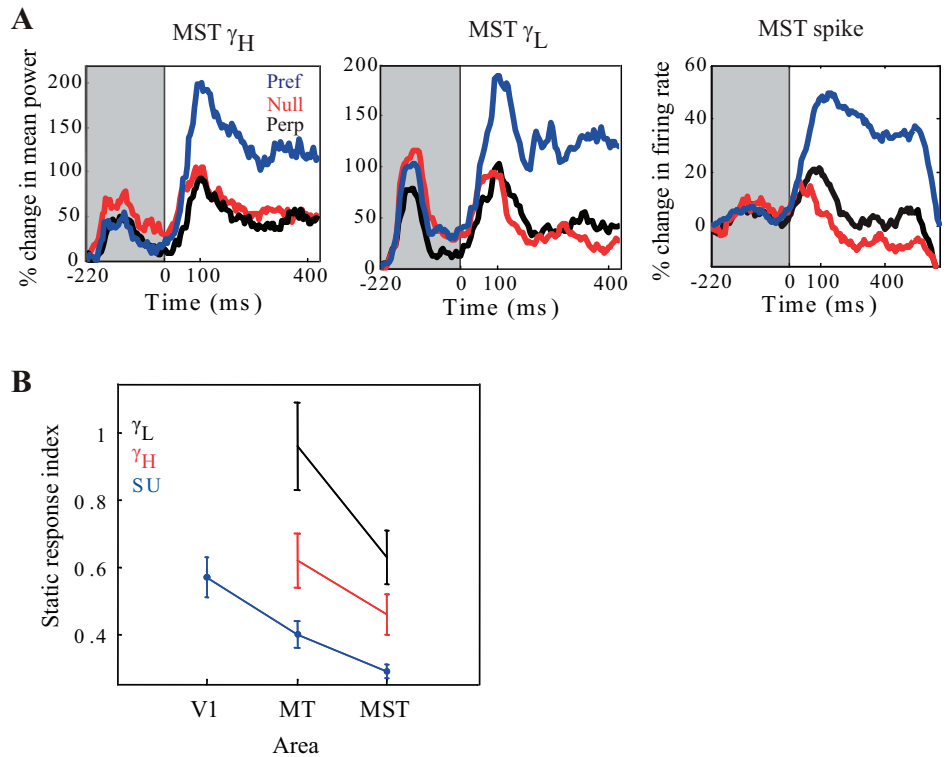
Fig. 4. Summary of local field potential (LFP) and spike responses to stationary stimuli. *A*: mean PSTHs illustrating the change in response for the population of MST high-gamma (γ_H) sites (*left*), low-gamma (γ_L) sites (*center*), and spikes (*right*) elicited by sinusoidal gratings. Preferred, null, and perpendicular directions are shown. Gratings were presented at −200 ms, remained stationary for 200 ms, and then began moving at 0 ms. The response evoked by the stationary stimulus is highlighted in gray. *B*: summary of the mean static response index (see METHODS) for γ_H, γ_L, and spike responses [single unit (SU)] for the population of V1, MT, and MST sites.

between V1 and both MT and MST (ANCOVA, $P < 0.001$) and marginally significant between MT and MST (ANCOVA, $P < 0.08$). Thus increases in tuning bandwidth were associated with similar increases in pattern selectivity in each area, and for a given tuning bandwidth pattern selectivity was stronger in MT and MST than in V1. Although the same tendency was present between MT and MST, it did not reach statistical significance, as would be expected had we obtained a larger sample size (Lagae et al. 1994). These results, along with those related to static motion responses, are consistent with the idea that the computation of pattern selectivity relies on similar mechanisms in each area. By both measures, however, the overall differences between V1 and MT were greater than those between MT and MST.

Processing of unikinetic plaids. As shown in Figs. 2 and 3, the responses to static orientations decrease at each stage along the dorsal visual pathway. However, previous theoretical and psychophysical work has shown that, under some circumstances, a static grating can be used to constrain the interpretation of motion. This results from the fact that a static grating is locally consistent with motion in a direction parallel to the grating's orientation (Albright 1984; Dobkins et al. 1998; Ferrera and Wilson 1990; Gorea and Lorenceau 1991). A clear example of this effect occurs with a unikinetic plaid, in which a stationary grating is superimposed on a moving one (Ferrera and Wilson 1990). In that case, one perceives motion parallel to the grating orientation, even though the static grating contains no time-varying information. Thus one might expect higher levels of the motion processing hierarchy to exhibit direction-selective biases to stimuli that contain stationary gratings, even though the responses to these stimuli presented in isolation decrease sharply at each stage.

To examine this issue, we recorded the responses of MT and MST neurons to bikinetic (Fig. 1*A*) and unikinetic (Fig. 1*B*)

plaid stimuli. Again the responses were quantified according to standard techniques (see METHODS) that classify neurons as "component," "pattern," or "unclassified" (Ferrera and Wilson 1990; Movshon et al. 1985; Smith et al. 2005). For unikinetic plaids, the component prediction is formed by adding together the responses of the moving grating and the static grating (see METHODS) (Fig. 5). The pattern prediction for the direction of unikinetic plaids is based on the velocity-space intersection of the two components, which corresponds to a clockwise rotation of the single grating tuning curve by 30°.

Figure 5 provides examples of MT and MST direction tuning curves for gratings as well as bikinetic and unikinetic plaids. Two typical MT neurons are illustrated (Fig. 5, *A* and *B*), along with one typical MST neuron (Fig. 5*C*). The polar plots show the observed responses in black, the component predictions in blue, and the pattern predictions in red. Below each tuning curve is shown the corresponding classification. Figure 5, *left* and *center*, show the responses and predictions to gratings and bikinetic plaids, respectively, while Fig. 5, *right*, corresponds to unikinetic plaids.

The first example neuron shown for MT (Fig. 5*A*) is categorized as "unclassified" (pattern index = 0) when stimulated with bikinetic plaids (Fig. 5*A*, *center*); however, it exhibits significant component selectivity when tested with unikinetic plaids (PI = −1.66; Fig. 5*A*, *right*). The MT neuron shown in Fig. 5*B* is categorized as a pattern cell when bikinetic plaids are used (PI = 3.24), but it is statistically unclassified for unikinetic plaids (PI = 0.25; Fig. 5*B*, *right*). Thus pattern selectivity decreases when both MT neurons are tested with unikinetic plaids. In contrast, the MST neuron, which is classified as pattern selective when stimulated with bikinetic plaids (PI = 5.08), also exhibits pattern selectivity when tested with unikinetic plaids (PI = 2.17; Fig. 5*C*, *right*).
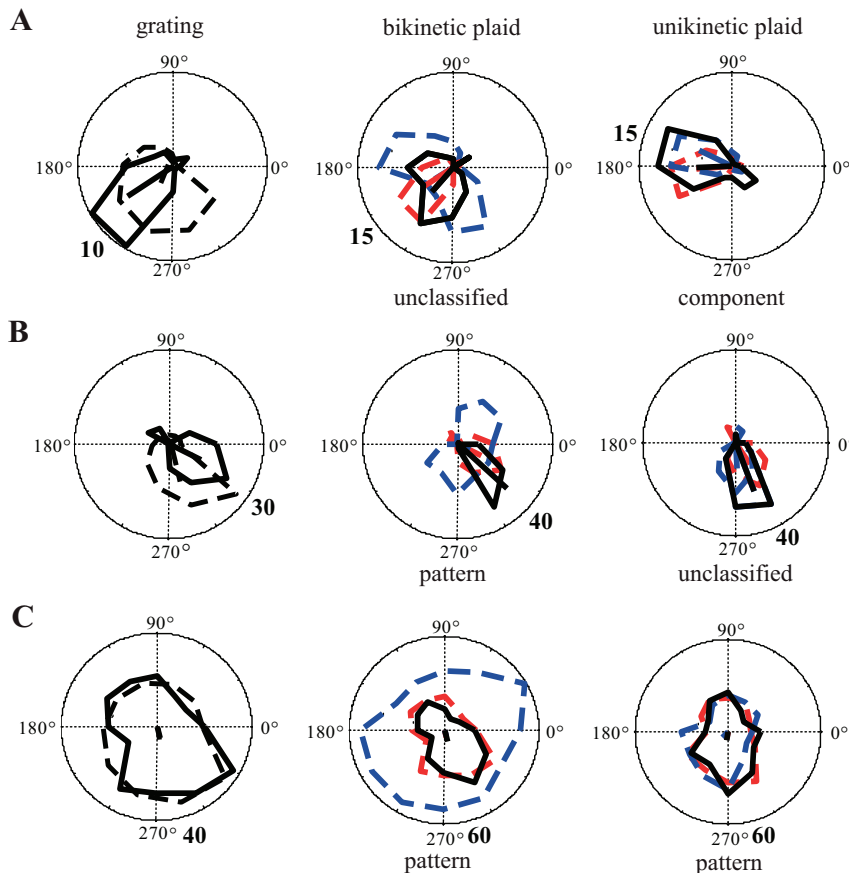
Fig. 5. Example spike responses of MT and MST neurons to bikinetic and unikinetic plaid stimuli. Polar plots showing examples of grating (*left*), bikinetic plaid (*center*), and unikinetic plaid (*right*) direction-tuning curves obtained from single recordings for a MT cell that is unclassified for bikinetic plaids but component tuned for unikinetic plaids (*A*), an MT cell that exhibits pattern selectivity with bikinetic plaids and is categorized as unclassified with unikinetic plaids (*B*), and an MST cell that is pattern selective with both bikinetic and unikinetic plaids (*C*). Neuronal responses are shown in solid black, direction-tuning curve fits in dashed black, component predictions in dashed blue, and pattern predictions in dashed red. The category (i.e., component, unclassified, or pattern) of each response for bikinetic and unikinetic plaids is provided below the corresponding polar plots.

Figure 6 plots the distributions of cell types for the MT (Fig. 6*A*, *left*) and MST (Fig. 6*B*, *left*) populations in response to bikinetic and unikinetic plaids. As reported previously (Khawaja et al. 2009), pattern selectivity for bikinetic plaids was greater in MST than in MT ($P < 0.05$; Student's *t*-test), and a similar difference is found for unikinetic plaids ($P < 0.05$; Student's *t*-test) (Fig. 6, *center*). As illustrated in Fig. 6, *center*, pattern selectivity was significantly lower in both MT and MST when unikinetic plaid stimuli were used [MT mean PI $= 0.002 \pm 0.35$ for bikinetic plaids vs. -1.36 ± 0.32 for unikinetic plaids ($P < 0.01$), MST mean PI $= 1.31 \pm 0.25$ for bikinetic plaids vs. -0.24 ± 0.27 for unikinetic plaids ($P < 0.001$); paired Student's *t*-test]. Similar results were obtained when we allowed for potential changes in the gain of the response to the static orientation during the motion period [MT mean PI -1.61 ± 0.35 for unikinetic plaids ($P < 0.01$), MST mean PI $= -0.65 \pm 0.32$ for unikinetic plaids ($P < 0.001$); see METHODS for model].

Figure 6, *right*, plots the PIs for the responses to bikinetic and unikinetic plaids in MT and MST. As suggested from Fig. 6, *center*, many neurons that are classified as pattern selective for bikinetic plaids are either classified as component selective or belong to the unclassified category when tested with unikinetic plaids [11/12 (92%) for MT and 15/22 (68%) for MST]. The decrease in the frequency of pattern selectivity is likely to be due in part to the difficulty of distinguishing between the pattern and component predictions, which are necessarily very similar for unikinetic plaids (Fig. 5). Because of the nature of the partial correlation coefficient used to define pattern selectivity, even slight departures from the component and pattern

predictions will cause neurons to be labeled as unclassified. However, the substantial increase in significant component selectivity in both MT and MST is not likely to be a consequence of this procedure, suggesting that responses to unikinetic plaids are genuinely less pattern selective in both areas. Overall, these areas appear to be different in their ability to integrate unikinetic plaids, as MST contains a significantly larger percentage of cells that are pattern selective for both types of plaid stimuli [Fig. 6, *A* and *B*, *right*, *top right* box of both panels: 7/22 (32%) in MST vs. 1/12 (8%) in MT; $P < 0.01$, binomial test]. Thus, although pattern selectivity is generally weaker for unikinetic plaids, area MST appears to be unique among the areas we examined in having appreciable proportion of neurons capable of robustly signaling pattern motion for different types of stimuli.

In contrast to our results with bikinetic plaids, there was no relationship between unikinetic pattern selectivity and the response to stationary stimuli in MST or MT (linear regression, $r^2 = 0.07$, $P = 0.28$ for MST and $r^2 = 0.008$, $P = 0.69$ for MT). Indeed, as mentioned above, responses to these static stimuli in MST were very low in amplitude and largely unselective, even though information about orientation is necessary to estimate the motion of the unikinetic plaid. Similarly, there was no clear relationship between tuning bandwidth and unikinetic plaid pattern selectivity in MT or MST (linear regression, $r^2 = 0.04$, $P = 0.23$ for MST and $r^2 = 0.04$, $P = 0.16$ for MT).

Unikinetic plaid temporal dynamics. Previous work has shown that the pattern selectivity of MT neurons for bikinetic plaids generally increases during the early phases of the re-
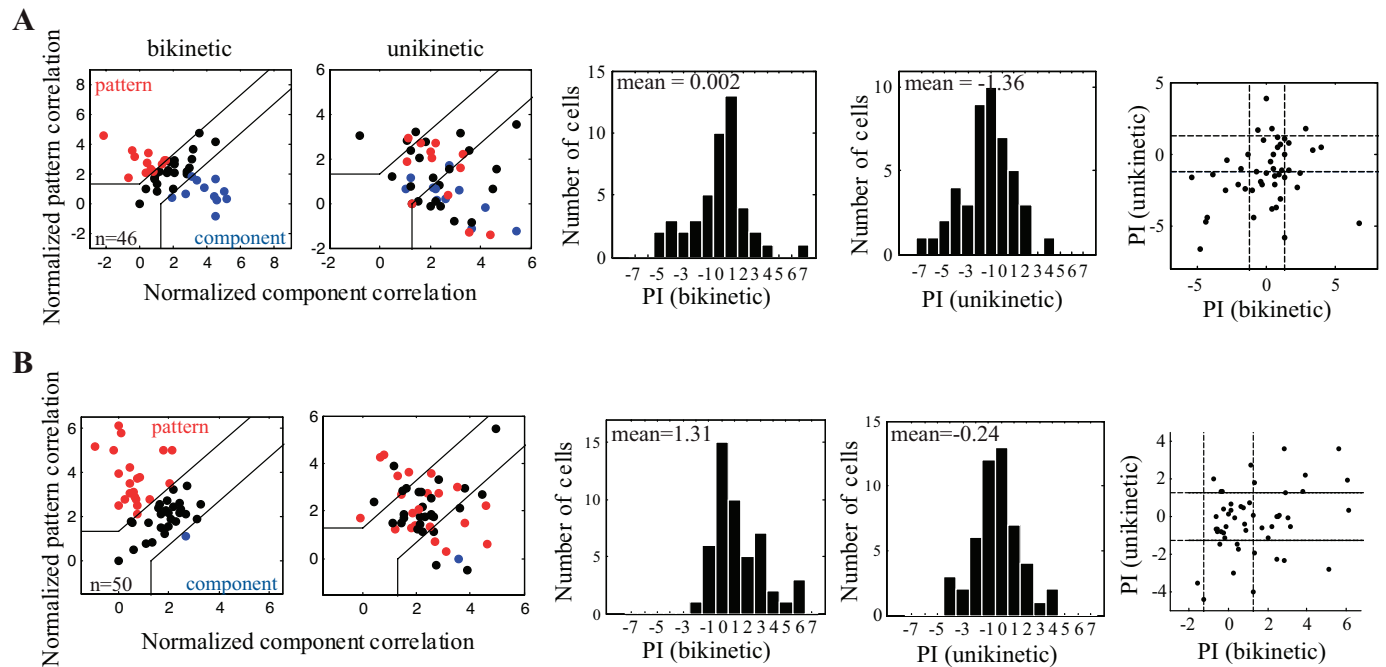
Fig. 6. Pattern and component selectivity in MT and MST for bikinetic and unikinetic plaids. *Left*: scatterplots showing Z-transformed component correlations vs. Z-transformed pattern correlations for the population of spikes recorded from MT (*A*; *n* = 46) and MST (*B*; *n* = 50). Cells were classified as pattern selective (red) and component selective (blue) according to the Z partial correlation coefficients between the data and the component and pattern predictions (see METHODS). Cells that could not be assigned to either category were labeled unclassified (black). *Center*: histograms showing a significantly smaller mean PI when unikinetic plaids are used for MT (*A*; *P* < 0.01) and MST (*B*; *P* < 0.001). The mean PI is greater for the MST population compared with the MT population when both bikinetic (*P* < 0.01) and unikinetic plaids (*P* < 0.05) are used. *Right*: scatterplots comparing the distribution of PIs for MT (*A*) and MST (*B*) for bikinetic vs. unikinetic plaids. MST contains a greater percentage of neurons that exhibit pattern selectivity for both types of plaid stimuli.

sponse (Pack et al. 2001; Pack and Born 2001; Smith et al. 2005; Solomon et al. 2012). Perceptually, the perceived direction of plaid stimuli approximates a vector average (or sum) of the motion components for brief presentation durations (Yo and Wilson 1992), with longer durations leading to the perception of pattern motion. The vector average and pattern direction are identical for bikinetic plaids, but for unikinetic plaids the two directions differ by the angle between the grating components. This difference has been exploited in ocular following experiments, which show that the initial eye movement responses to unikinetic plaids exhibit a clear temporal transition in both humans and monkeys (Barthelemy et al. 2010; Masson and Castet 2002). Specifically, these studies show that eye movement responses to a unikinetic plaid stimulus initially follow the moving grating and only incorporate the static grating after a delay. Consequently, the latency for initiating accurate tracking movements for unikinetic plaids is somewhat longer than that for tracking gratings or bikinetic plaids.

To investigate the temporal dynamics of neural responses to unikinetic plaids, we plotted the mean PI as a function of time for both MT and MST. In these plots the PI accumulates across time (Smith et al. 2005) (see METHODS). Figure 7*A* shows that, for bikinetic stimuli, the average time required for pattern-selective neurons to become statistically pattern selective is similar for MT (mean = 143 ± 12 ms; *n* = 12) and MST (mean = 150 ms ± 11.33 ms; *n* = 12) (*P* = 0.68; Student's *t*-test). Consistent with the results on ocular following, pattern selectivity emerges substantially later for unikinetic plaids, with a delay that is similar for the two areas [Fig. 7*B*; PI mean time = 225 ± 71.90 for MT (*n* = 4) vs. 255 ± 67.07 for MST

(*n* = 24); *P* = 0.77, Student's *t*-test]. To emphasize this difference, Fig. 7, *C* and *D*, replot the time course of pattern selectivity for unikinetic plaids and for bikinetic plaids in MT and MST, respectively. In MT the latency of pattern selectivity was longer for unikinetic than for bikinetic plaid stimuli, although this difference did not reach significance (*P* = 0.14; Student's *t*-test). In MST the computation of pattern selectivity for unikinetic plaids lagged that for bikinetic plaids, and this difference was statistically significant (*P* < 0.05; Student's *t*-test). The results we have observed in MST are thus consistent with previous studies that show that eye movement responses to unikinetic plaids initially correspond to the moving grating and incorporate the static grating later in time (Masson and Castet 2002).

Correlates with perceptual transparency. Our results up to this point suggest that MST neurons are more pattern selective than neurons in previous areas for both bikinetic and unikinetic plaids. This is consistent with the idea that neuronal responses at higher stages are more strongly correlated with visual perception than those at lower levels (Williams et al. 2003). However, an alternative interpretation is that the higher-level neurons are simply more effective at integrating motion signals, as evidenced by the increase in receptive field size and tuning bandwidth at successive stages along the pathway. These two possibilities (greater integration vs. correlation with perception) lead to the same outcome when the stimulus is a coherent bikinetic or unikinetic plaid, but they predict divergent results for other types of stimuli.

A particularly interesting example is the transparent plaid stimulus introduced by Stoner et al. (Stoner and Albright 1992; Stoner et al. 1990). This stimulus is similar to the plaid stimuli
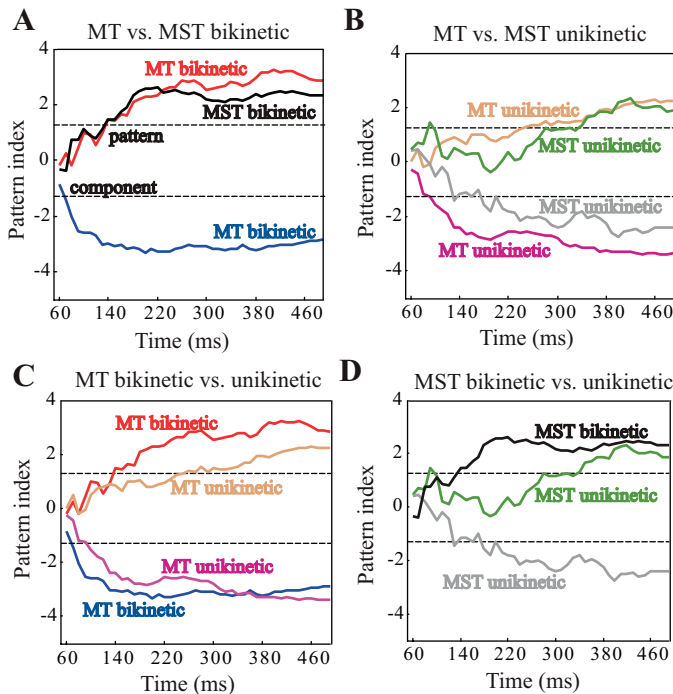
Fig. 7. Temporal dynamics of component and pattern selectivity. *A*: temporal dynamics of the mean PI when bikinetic plaids are used for the set of MT component (blue) and pattern (red) neurons and for MST pattern neurons (black) in our sample. Dashed black lines demarcate the threshold of PI used to consider a neuron as component (−1.28) or pattern (+1.28) selective. *B*: average temporal response profile of MT component (purple) and pattern (light brown) neurons as well as MST component (gray) and pattern (green) neurons. *C*: mean time course of MT component and pattern selectivity for both bikinetic and unikinetic plaids. *D*: mean time course of MST component and pattern selectivity for both bikinetic and unikinetic plaids.

described in the previous section, except that the plaid is displayed against a bright background and each of the component gratings is made to appear translucent. Thus where the gratings intersect, the luminance is no longer additive but instead conforms to the laws of transparency (Metelli 1974). Mathematically the nonadditivity of the intersections can, under certain assumptions, introduce motion signals in the pattern direction, but perceptually the resulting motion is more consistent with the motion of the components. That is, observers perceive the two gratings to be sliding over each other, rather than seeing a single pattern moving coherently (Stoner et al. 1990).

The transparent plaid stimulus allows us to dissociate two possible explanations for the increased pattern selectivity observed in MST with both unikinetic and bikinetic plaids. The responses of MST cells that have outputs that are most similar to human perception should become more component-like for transparent stimuli, and this modulation should be stronger than that observed in MT. On the other hand, if MST cells are simply integrating motion components indiscriminately, then we should see little effect of the transparent manipulation. We tested these possibilities on 37 V1 cells, 52 MT cells, and 69 MST cells.

Each cell was tested with an additive square-wave plaid (which is perceptually coherent) and a nonadditive, perceptually transparent, plaid. Figure 8*A* plots the values of the PI for the two different kinds of plaid tested on each cell. For area V1 (Fig. 8*A*), these values tend to fall along the unity line,

indicating no modulation by perceptual transparency. For MT (Fig. 8*B*), consistent with previous results (Stoner and Albright 1992), the points tend to fall below the unity line, suggesting that these responses are modulated by depth cues associated with transparency. Surprisingly, there is on average little modulation by transparency in MST, as the points in Fig. 8*C* tend again to fall along the unity line.

To quantify the degree of transparent modulation in each neuron, we defined a transparency index (TI) by subtracting the component index obtained in the coherent condition from that obtained in the transparent condition. Thus more negative values of TI indicate greater modulation by transparency. Transparency modulation significantly increases from V1 to MT (mean of 0.02 in V1 and −0.67 in MT; $P < 0.05$, Student's *t*-test), but a similar increase is not observed in the comparison between MT and MST (mean of −0.67 in MT and 0.02 in MST; $P < 0.01$, Student's *t*-test). Of the three areas tested, transparency modulation was significantly different from zero only in MT ($P < 0.001$, Student's *t*-test). Indeed, there is little overall modulation by transparency in the MST population (mean TI = 0.02), consistent with the hypothesis that MST cells integrate motion components indiscriminately.

One possible explanation for these results is that our recordings targeted dorsal MST (MSTd) rather than ventral MST (MSTv). This is entirely possible, as many of the neurons described here came from a previous study aimed at examining optic flow processing (Mineault et al. 2012), which is a key
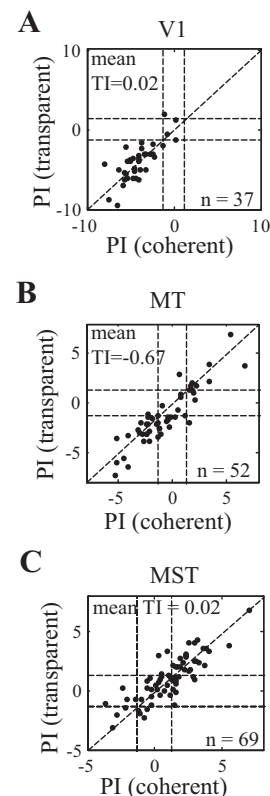

Fig. 8. Pattern selectivity of the population of V1, MT, and MST neuronal responses to coherent vs. transparent plaids: comparison of the distribution of PIs measured for V1 (*A*; 37 cells), MT (*B*; 52 cells), and MST (*C*; 69 cells) neuronal responses to coherent (*x*-axis) vs. transparent (*y*-axis) plaids. The mean transparency index (TI) for V1 is significantly smaller than that for MT ($P < 0.05$), which is significantly larger than that found in MST ($P < 0.01$).

function of MSTd. In contrast, MSTv is thought to be involved in object motion processing, a task that may require the use of information about transparency (Britten 2008). Although we have no definitive method of identifying the anatomical locations of the neurons from which we recorded, previous work has shown that MSTv neurons exhibit greater surround-suppression than MSTd neurons (Eifuku and Wurtz 1998). However, we found no correlation between the TI and a measure of surround-suppression in MST (linear regression; $P > 0.74$).

DISCUSSION

In this work we have characterized the responses of MST neurons to visual stimuli that have classically been used to study motion selectivity in earlier cortical areas, such as V1 and MT. Previous research on pattern motion selectivity in these areas has led to the notion of a two-stage model in which the projection from V1 to MT is largely responsible for estimates of object velocity that are invariant to other stimulus parameters, notably orientation. Our results, while generally consistent with the hierarchical aspect of these models, suggest that the relevant computations involve additional areas, including MST. Indeed, our results with unikinetic plaids provide an example of a pattern motion computation that is unlikely to be carried out fully at the level of MT. For these stimuli the relationship between MT and MST is qualitatively similar to that between V1 and MT for bikinetic plaids: MT neurons are generally selective for the motion components, while a minority of MST neurons are capable of signaling pattern motion.

Mechanisms of motion integration. The estimation of object motion is often characterized as a two-stage process, in which the second stage infers the velocity of the object from first-stage measurements that are individually ambiguous. The ambiguity results in part from the fact that motion-selective neurons in areas such as V1 will respond to a stationary stimulus nearly as strongly as they respond to one that moves in their preferred motion direction (see, for example, Fig. 2*A*). Such responses are obviously problematic for an organism that relies on these neurons to estimate motion. In theory, this problem can be solved by subtracting the outputs of two neurons tuned to opposite motion directions (Adelson and Bergen 1985; Reichardt 1961; van Santen and Sperling 1985), as the portion of the response due to the stationary stimulus will on average be equal in both cells. The process that carries out the subtraction is called a motion-opponent mechanism.

A similar ambiguity exists for moving stimuli. For a stimulus composed of multiple contours, the response of a neuron in V1 will generally depend on the shape of the object as well as its velocity. This confound results from the fact that neurons with small receptive fields only receive information about the component of motion perpendicular to the orientation of a contour passing through their receptive fields (Wallach 1935). One way to resolve this problem is to implement a second stage that integrates over the outputs of multiple first-stage neurons that prefer different motion directions (Rust et al. 2006; Simoncelli and Heeger 1998; Welch 1989).

Our results, consistent with previous findings (Qian and Andersen 1994; Rust et al. 2006), indicate that both the strength of opponent motion processing and the bandwidth of integration are greater in MT than in V1. We also find that both mechanisms are stronger in MST than in MT, suggesting that

these fundamental aspects of motion integration are carried out in at least three stages along the dorsal visual hierarchy. A comparative analysis of our data from V1, MT, and MST (Fig. 3) indicates that the increases in motion opponency and tuning bandwidth are not by themselves sufficient to account for the increased pattern selectivity seen at higher-level areas of the cortex. Rather, pattern selectivity is generally greater in MST than in MT and in MT than in V1, even when the increase in the mean tuning bandwidth and decrease in responses to static stimuli are taken into account (Fig. 3).

Implications for motion models. Both of the mechanisms discussed above (opponent motion and integration) can be modeled as linear operations, in which the inputs of one stage are added or subtracted to generate the output of the next stage. While these linear operations are incorporated to some degree into virtually all models of motion processing, recent models also include a nonlinear operation that transforms the outputs of each of the neurons at one stage prior to their summation at the next stage. Thus, for example, an MT neuron can effectively be modeled as receiving input from a number of V1 neurons, with each input being transformed by a nonlinear function prior to summation at the MT stage. Generally the nonlinear transformation is captured by a compressive function, which causes the contribution of each neuron to saturate (Nishimoto and Gallant 2011; Rust et al. 2006; Tsui et al. 2010). Interestingly, the same nonlinearity was recently shown to be essential to account for the transformation of optic flow selectivity between MT and MST (Mineault et al. 2012). Thus a generic model that makes use of similar linear and nonlinear mechanisms seems capable of accounting for selectivity in both MT and MST for various stimuli including plaids (Rust et al. 2006; Tsui et al. 2010), optic flow (Mineault et al. 2012), and natural scenes (Nishimoto and Gallant 2011).

One departure from this generic modeling framework concerns the mechanisms underlying the processing of unikinetic plaids. From a theoretical standpoint, these stimuli are particularly challenging because they require the estimate of motion direction to take into account information from nonmoving stimuli that by themselves elicit little neuronal response. In the case of the unikinetic plaid the velocity of the pattern is perceived to be parallel to the nonmoving grating component. In our data (Fig. 6), pattern selectivity for unikinetic plaids was most common in area MST, where responses to such static stimuli were negligible. Thus models that rely entirely on the mechanisms discussed above (motion opponency, integration across motion directions, nonlinear transformations of firing rates) are unlikely to account for this selectivity. Instead, the existence of cells that are pattern selective for both unikinetic and bikinetic plaids would seem to require more specialized mechanisms, such as an intersection-of-constraints calculation (Simoncelli and Heeger 1998) or a mechanism for integrating second-order motion signals (Ferrera and Wilson 1990). Although limited evidence for both mechanisms has been found in MT (Albright 1992; Nishimoto and Gallant 2011; Priebe et al. 2003), they remain largely unexplored in MST.

Transparency. As mentioned above in the context of unikinetic plaids, the interpretation of visual motion can be strongly influenced by visual cues that contain no time-varying information. One important example concerns depth cues, such as retinal disparity (Duncan et al. 2000; Shimojo et al. 1989), occlusion (Pack et al. 2004; Vallortigara and Bressan 1991),

and transparency (Stoner et al. 1990; Stoner and Albright 1992). The influence of the latter cue is particularly evident when luminance conditions are used to manipulate the apparent depth arrangement of the components of a plaid stimulus (Stoner et al. 1990).

Consistent with previous results (Stoner and Albright 1992), we have found a neuronal correlate of these perceptual findings in MT. Our results further suggest that modulation of neuronal responses by transparency is lacking in V1 (Fig. 8), where neurons generally respond to the individual component gratings even for perceptually coherent plaids. These results together might suggest that neurons further along the dorsal pathway combine motion and depth signals in a manner that is more consistent with perception, but we found little evidence for this idea. Indeed, the responses of the MST population to transparent plaids were similar to those of the V1 population. This would seem to contradict previous findings that MST responses are more consistent with visual perception (Williams et al. 2003); here we consider a number of possible ways to interpret this result.

The first possibility is that the perception of transparent plaid stimuli may involve pathways that do not include the MST neurons in our sample. Indeed, as mentioned in RESULTS, our recordings targeted area MSTd, which is often assumed to be associated with self-motion rather than object motion processing (Tanaka et al. 1993). We consider this to be an unlikely explanation, because computational results have shown that MSTd neurons are in fact capable of estimating object motion (Mineault et al. 2012; Zemel and Sejnowski 1998). Moreover, transparency cues are likely to improve estimates of self-motion and to modulate the responses of MSTd neurons (Upadhyay et al. 2000).

A second possibility is that the stimuli used in our experiments were not perceptually transparent. Although we selected stimulus parameters that induced strong percepts of transparency in humans (Stoner et al. 1990), we did not attempt to optimize them for the monkeys in our study. Although one previous report suggests that the perception of transparent plaids is similar between macaques and humans (Thiele and Stoner 2003), there are considerable technical problems associated with training monkeys to report their percepts of these stimuli. Thus we cannot rule out this possibility completely.

A third possible explanation for our results is that transparency modulation is present in MST but not apparent at the single-unit level. This would result if the neural correlate of transparency population involved synchrony among neurons (Castelo-Branco et al. 2000) or if it involved a more specialized readout of the neuronal population (Treue et al. 2000). The former is theoretically possible, although a direct test of the relationship between stimulus transparency and synchrony in the awake monkey failed to find the predicted result (Thiele and Stoner 2003). The other possibility, that transparency perception results from the precise shape of the overall distribution of responses in a population (Treue et al. 2000), remains entirely possible. Indeed, the broad tuning of individual MST neurons for motion direction and spatial position would seem to necessitate additional processing to extract the motion of multiple, independently moving objects.

DISCLOSURES

No conflicts of interest, financial or otherwise, are declared by the author(s).

AUTHOR CONTRIBUTIONS

Author contributions: F.A.K. and L.D.L. performed experiments; F.A.K. analyzed data; F.A.K. and C.C.P. interpreted results of experiments; F.A.K. prepared figures; F.A.K. and C.C.P. drafted manuscript; F.A.K. and C.C.P. edited and revised manuscript; F.A.K., L.D.L., and C.C.P. approved final version of manuscript; C.C.P. conception and design of research.

REFERENCES

Adelson EH, Bergen JR. Spatiotemporal energy models for the perception of motion. *J Opt Soc Am A* 2: 284–299, 1985.

Adelson EH, Movshon JA. Phenomenal coherence of moving visual patterns. *Nature* 300: 523–525, 1982.

Albright TD. Direction and orientation selectivity of neurons in visual area MT of the macaque. *J Neurophysiol* 52: 1106–1130, 1984.

Albright TD. Form-cue invariant motion processing in primate visual cortex. *Science* 255: 1141–1143, 1992.

Barthelemy FV, Fleuriet J, Masson GS. Temporal dynamics of 2D motion integration for ocular following in macaque monkeys. *J Neurophysiol* 103: 1275–1282, 2010.

Born RT. Center-surround interactions in the middle temporal visual area of the owl monkey. *J Neurophysiol* 84: 2658–2669, 2000.

Britten KH. Mechanisms of self-motion perception. *Annu Rev Neurosci* 31: 389–410, 2008.

Cadieu C, Kouh M, Pasupathy A, Connor CE, Riesenhuber M, Poggio T. A model of V4 shape selectivity and invariance. *J Neurophysiol* 98: 1733–1750, 2007.

Castelo-Branco M, Goebel R, Neuenschwander S, Singer W. Neural synchrony correlates with surface segregation rules. *Nature* 405: 685–689, 2000.

Churchland AK, Huang X, Lisberger SG. Responses of neurons in the medial superior temporal visual area to apparent motion stimuli in macaque monkeys. *J Neurophysiol* 97: 272–282, 2007.

Churchland MM, Priebe NJ, Lisberger SG. Comparison of the spatial limits on direction selectivity in visual areas MT and V1. *J Neurophysiol* 93: 1235–1245, 2005.

Connor CE, Brincat SL, Pasupathy A. Transformation of shape information in the ventral pathway. *Curr Opin Neurobiol* 17: 140–147, 2007.

Dobkins KR, Stoner GR, Albright TD. Perceptual, oculomotor, and neural responses to moving color plaids. *Perception* 27: 681–709, 1998.

Duffy CJ, Wurtz RH. Sensitivity of MST neurons to optic flow stimuli. I. A continuum of response selectivity to large-field stimuli. *J Neurophysiol* 65: 1329–1345, 1991a.

Duffy CJ, Wurtz RH. Sensitivity of MST neurons to optic flow stimuli. II. Mechanisms of response selectivity revealed by small-field stimuli. *J Neurophysiol* 65: 1346–1359, 1991b.

Duncan RO, Albright TD, Stoner GR. Occlusion and the interpretation of visual motion: perceptual and neuronal effects of context. *J Neurosci* 20: 5885–5897, 2000.

Eifuku S, Wurtz RH. Response to motion in extrastriate area MSTl: center-surround interactions. *J Neurophysiol* 80: 282–296, 1998.

Ferrera VP, Wilson HR. Perceived direction of moving two-dimensional patterns. *Vision Res* 30: 273–287, 1990.

Geesaman BJ, Andersen RA. The analysis of complex motion patterns by form/cue invariant MSTd neurons. *J Neurosci* 16: 4716–4732, 1996.

Gizzi MS, Katz E, Schumer RA, Movshon JA. Selectivity for orientation and direction of motion of single neurons in cat striate and extrastriate visual cortex. *J Neurophysiol* 63: 1529–1543, 1990.

Gorea A, Lorenceau J. Directional performances with moving plaids: component-related and plaid-related processing modes coexist. *Spat Vis* 5: 231–252, 1991.

Graziano MS, Andersen RA, Snowden RJ. Tuning of MST neurons to spiral motions. *J Neurosci* 14: 54–67, 1994.

Henrie JA, Shapley R. LFP power spectra in V1 cortex: the graded effect of stimulus contrast. *J Neurophysiol* 94: 479–490, 2005.

Hubel DH, Wiesel TN. Receptive fields and functional architecture of monkey striate cortex. *J Physiol* 195: 215–243, 1968.

Hubel DH, Wiesel TN. Receptive fields, binocular interaction and functional architecture in the cat's visual cortex. *J Physiol* 160: 106–154, 1962.

Khawaja FA, Tsui JM, Pack CC. Pattern motion selectivity of spiking outputs and local field potentials in macaque visual cortex. *J Neurosci* 29: 13702–13709, 2009.

Kouh M, Poggio T. A canonical neural circuit for cortical nonlinear operations. *Neural Comput* 20: 1427–1451, 2008.

Lagae L, Maes H, Raiguel S, Xiao DK, Orban GA. Responses of macaque STS neurons to optic flow components: a comparison of areas MT and MST. *J Neurophysiol* 71: 1597–1626, 1994.

Masson GS, Castet E. Parallel motion processing for the initiation of short-latency ocular following in humans. *J Neurosci* 22: 5149–5163, 2002.

Maunsell JH, Van Essen DC. Functional properties of neurons in middle temporal visual area of the macaque monkey. I. Selectivity for stimulus direction, speed, and orientation. *J Neurophysiol* 49: 1127–1147, 1983.

Metelli F. The perception of transparency. *Sci Am* 230: 90–98, 1974.

Mikami A, Newsome WT, Wurtz RH. Motion selectivity in macaque visual cortex. I. Mechanisms of direction and speed selectivity in extrastriate area MT. *J Neurophysiol* 55: 1308–1327, 1986.

Miles FA. Visual stabilization of the eyes in primates. *Curr Opin Neurobiol* 7: 867–871, 1997.

Mineault PJ, Khawaja FA, Butts DA, Pack CC. Hierarchical processing of complex motion along the primate dorsal visual pathway. *Proc Natl Acad Sci USA* 109: E972–E980, 2012.

Movshon JA, Adelson EH, Gizzi MS, Newsome WT. The analysis of visual moving patterns. In: *Pattern Recognition Mechanisms*, edited by Chagas C, Gatass R, Gross C. New York: Springer, 1985, p. 117–151.

Nishimoto S, Gallant JL. A three-dimensional spatiotemporal receptive field model explains responses of area MT neurons to naturalistic movies. *J Neurosci* 31: 14551–14564, 2011.

Pack CC, Berezovskii VK, Born RT. Dynamic properties of neurons in cortical area MT in alert and anaesthetized macaque monkeys. *Nature* 414: 905–908, 2001.

Pack CC, Born RT. Temporal dynamics of a neural solution to the aperture problem in visual area MT of macaque brain. *Nature* 409: 1040–1042, 2001.

Pack CC, Conway BR, Born RT, Livingstone MS. Spatiotemporal structure of nonlinear subunits in macaque visual cortex. *J Neurosci* 26: 893–907, 2006.

Pack CC, Gartland AJ, Born RT. Integration of contour and terminator signals in visual area MT of alert macaque. *J Neurosci* 24: 3268–3280, 2004.

Palanca BJ, DeAngelis GC. Macaque middle temporal neurons signal depth in the absence of motion. *J Neurosci* 23: 7647–7658, 2003.

Priebe NJ, Cassanello CR, Lisberger SG. The neural representation of speed in macaque area MT/V5. *J Neurosci* 23: 5650–5661, 2003.

Qian N, Andersen RA. Transparent motion perception as detection of unbalanced motion signals. II. Physiology. *J Neurosci* 14: 7367–7380, 1994.

Regan D. Visual factors in hitting and catching. *J Sports Sci* 15: 533–558, 1997.

Reichardt W. Autocorrelation, a principle for the evaluation of sensory information by the central nervous system. In: *Sensory Communication*, edited by Rosenblith WA. Cambridge, MA: MIT Press, 1961, p. 303–317.

Rust NC, Dicarlo JJ. Selectivity and tolerance ("invariance") both increase as visual information propagates from cortical area V4 to IT. *J Neurosci* 30: 12978–12995, 2010.

Rust NC, Mante V, Simoncelli EP, Movshon JA. How MT cells analyze the motion of visual patterns. *Nat Neurosci* 9: 1421–1431, 2006.

Saito H, Yukie M, Tanaka K, Hikosaka K, Fukada Y, Iwai E. Integration of direction signals of image motion in the superior temporal sulcus of the macaque monkey. *J Neurosci* 6: 145–157, 1986.

Shimojo S, Silverman GH, Nakayama K. Occlusion and the solution to the aperture problem for motion. *Vision Res* 29: 619–626, 1989.

Simoncelli EP, Heeger DJ. A model of neuronal responses in visual area MT. *Vision Res* 38: 743–761, 1998.

Smith MA, Majaj NJ, Movshon JA. Dynamics of motion signaling by neurons in macaque area MT. *Nat Neurosci* 8: 220–228, 2005.

Solomon SS, Tailby C, Gharaei S, Camp AJ, Bourne JA, Solomon SG. Visual motion integration by neurons in the middle temporal area of a New World monkey, the marmoset. *J Physiol* 589: 5741–5758, 2012.

Stoner GR, Albright TD. Neural correlates of perceptual motion coherence. *Nature* 358: 412–414, 1992.

Stoner GR, Albright TD, Ramachandran VS. Transparency and coherence in human motion perception. *Nature* 344: 153–155, 1990.

Tanaka K, Hikosaka K, Saito H, Yukie M, Fukada Y, Iwai E. Analysis of local and wide-field movements in the superior temporal visual areas of the macaque monkey. *J Neurosci* 6: 134–144, 1986.

Tanaka K, Sugita Y, Moriya M, Saito H. Analysis of object motion in the ventral part of the medial superior temporal area of the macaque visual cortex. *J Neurophysiol* 69: 128–142, 1993.

Thiele A, Stoner G. Neuronal synchrony does not correlate with motion coherence in cortical area MT. *Nature* 421: 366–370, 2003.

Tinsley CJ, Webb BS, Barraclough NE, Vincent CJ, Parker A, Derrington AM. The nature of V1 neural responses to 2D moving patterns depends on receptive-field structure in the marmoset monkey. *J Neurophysiol* 90: 930–937, 2003.

Treue S, Hol K, Rauber HJ. Seeing multiple directions of motion-physiology and psychophysics. *Nat Neurosci* 3: 270–276, 2000.

Tsui JM, Hunter JN, Born RT, Pack CC. The role of V1 surround suppression in MT motion integration. *J Neurophysiol* 103: 3123–3138, 2010.

Upadhyay UD, Page WK, Duffy CJ. MST responses to pursuit across optic flow with motion parallax. *J Neurophysiol* 84: 818–826, 2000.

Vallortigara G, Bressan P. Occlusion and the perception of coherent motion. *Vision Res* 31: 1967–1978, 1991.

van Santen JP, Sperling G. Elaborated Reichardt detectors. *J Opt Soc Am A* 2: 300–321, 1985.

Wallach H. Uber visuell wahrgenommene Bewegungsrichtung. *Psychol Forsch* 20: 325–380, 1935.

Welch L. The perception of moving plaids reveals two motion-processing stages. *Nature* 337: 734–736, 1989.

Williams ZM, Elfar JC, Eskandar EN, Toth LJ, Assad JA. Parietal activity and the perceived direction of ambiguous apparent motion. *Nat Neurosci* 6: 616–623, 2003.

Yo C, Wilson HR. Moving two-dimensional patterns can capture the perceived directions of lower or higher spatial frequency gratings. *Vision Res* 32: 1263–1269, 1992.

Zemel RS, Sejnowski TJ. A model for encoding multiple object motions and self-motion in area MST of primate visual cortex. *J Neurosci* 18: 531–547, 1998.